

VŠB-Technická univerzita Ostrava  
Univerzitní studijní programy

Příprava a charakterizace fotoakatalyticky aktivního  
oxidu titaničitého

Preparation and characterization of titanium dioxide  
photocatalyst

Student: Jaroslav Lang

Vedoucí bakalářské práce: Ing. Vlastimil Matějka, Ph.D.

Datum odevzdání: 20.05.2011

## Diploma Thesis Assignment

Student: **Jaroslav Lang**  
Study Programme: B3942 Nanotechnology  
Study Branch: 3942R001 Nanotechnology  
Title: **Příprava a charakterizace fotokatalyticky aktivního oxidu titaničitého**  
**Preparation and characterization of titanium dioxide photocatalyst**

### Description:

The aim of proposed bachelor work is preparation and characterization of nanosized titanium dioxide. The nanoparticles will be prepared using a sol-gel method and titanium isopropoxide as titanium dioxide precursor will be used.

### Solution of the proposed work is divided into following steps:

1. Overview of the methods utilized for nanosized titanium dioxide preparation with emphasize on the sol-gel process.
2. Preparation of nanosized titanium dioxide using sol-gel method and titanium tetraisopropoxide as titanium dioxide precursor.
3. Evaluation of the photodegradation activity of the prepared titanium dioxide using photodegradation of model organic dye.

### References:

- CARP, O.; HUISMAN, C.L.; RELLER, A. Photoinduced reactivity of titanium dioxide. *Progress in Solid State Chemistry*. 2004, vol. 32, no. 1-2, s. 33 – 177.  
DIEBOLD, U. The surface science of titanium dioxide. *Surface Science Reports*. 2003, vol. 48, no. 5-8, s. 53-229.

Extent and terms of a thesis are specified in directions for its elaboration that are opened to the public on the web sites of the faculty.

Supervisor: **Ing. Vlastimil Matějka, Ph.D.**

Date of issue: 15.10.2010

Date of submission: 20.05.2011



prof. Ing. Jaromír Pištora, CSc.  
Head of Department

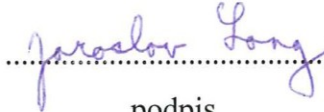


prof. Ing. Petr Noskovič, CSc.  
Vice-rector for Study Affairs

# Prohlášení

- Byl(a) jsem seznámen(a) s tím, že na moji bakalářskou práci se plně vztahuje zákon č.121/2000 Sb. - autorský zákon, zejména § 35 - využití díla v rámci občanských a náboženských obřadů, v rámci školních představení a využití díla školního a § 60 - školní dílo.
- Beru na vědomí, že Vysoká škola báňská - Technická univerzita Ostrava (dále jen VŠB-TUO) má právo nevýdělečně, ke své vnitřní potřebě, bakalářskou práci užít (§ 35 odst. 3).
- Souhlasím s tím, že jeden výtisk bakalářské práce bude uložen v Ústřední knihovně VŠB-TUO k prezenčnímu nahlédnutí a jeden výtisk bude uložen u vedoucího bakalářské práce. Souhlasím s tím, že údaje o bakalářské práci, obsažené v Záznamu o závěrečné práci, umístěném v příloze mé bakalářské práce, budou zveřejněny v informačním systému VŠB-TUO.
- Bylo sjednáno, že s VŠB-TUO, v případě zájmu z její strany, uzavřu licenční smlouvu s oprávněním užít dílo v rozsahu § 12 odst. 4 autorského zákona.
- Bylo sjednáno, že užít své dílo - bakalářskou práci nebo poskytnout licenci k jejímu využití mohu jen se souhlasem VŠB-TUO, která je oprávněna v takovém případě ode mne požadovat přiměřený příspěvek na úhradu nákladů, které byly VŠB-TUO na vytvoření díla vynaloženy (až do jejich skutečné výše).
- Místopřísežně prohlašuji, že celou bakalářskou práci včetně příloh, jsem vypracoval(a) samostatně a uvedl(a) jsem všechny použité podklady a literaturu.

V Ostravě dne 20.05. 2011

  
.....  
podpis

## ANOTACE BAKALÁŘSKÉ PRÁCE

LANG, J. *Příprava a charakterizace fotoakatalyticky aktivního oxidu titaničitého: bakalářská práce*. Ostrava : VŠB –Technická univerzita Ostrava, Univerzitní studijní programy, 2011, 43 s. Vedoucí práce: Matějka, V.

Bakalářská práce se zabývá přípravou a charakterizací fotoaktivního oxidu titaničitého. Nanostrukturovaný oxid titaničitý je významným fotokatalyzátorem využívaným v mnoha odvětvích od čištění vody až po jeho využití v energetickém průmyslu. Tato bakalářská práce se zabývá přípravou oxidu titaničitého metodou sol-gel. Jako prekurzor titanu byl použit isopropylalkoholát titaničitý, vzorky oxidu titaničitého byly připraveny ve formě prášku a ve formě tenkých vrstev nanesených metodou dip-coating na skleněných substrátech. Připravené vzorky byly charakterizovány vybranými metodami chemické a fázové analýzy, morfologie vzorků byla studována pomocí mikroskopických technik. U připravených materiálů byla testována jejich fotodegradační aktivita.

**Klíčová slova:** fotokatalyzátor, oxid titaničitý, isopropylalkoholát titaničitý, dip-coating

## ANNOTATION OF BACHELOR THESIS

LANG, J. *Preparation and characterization of titanium dioxide photocatalyst : Bachelor Thesis*. Ostrava : VŠB –Technical University of Ostrava, University Study Programmes, 2011, 43 p. Thesis supervisor: Matějka, V.

The bachelor thesis is focused on the preparation and characterization of photocatalytically active titanium dioxide. Nanostructured titanium dioxide is outstanding photocatalyst finding a variety of applications from the water treatment to its utilization in energetic. This bachelor thesis focuses on the preparation of the titanium dioxide using the sol-gel method. Titanium tetraisopropoxide was used as a titanium precursor. The samples were prepared in the form of powder as well as in the form of thin layers deposited on the glass substrate. The prepared samples were characterized using methods of chemical and phase analysis, the morphology of the samples was studied using microscopy techniques. The prepared samples were examined for evaluation of their photodegradation activity.

**Key words:** photocatalyst, titanium dioxide, titanium tetraisopropoxide, dip-coating

## List of abbreviations

AAS = Atomic absorption spectroscopy

AFM = Atomic force microscopy

CB = conductive band

CVD = chemical vapor deposition

EDX = Energy-dispersive X-ray spectroscopy

E<sub>g</sub> = band gap energy

ICP-OES = Optical emission spectrometry with inductively coupled plasma

L<sub>c</sub> = crystallite size

OE GDS = Optical emission glow discharge spectrometry

PVD = physical vapor deposition

SE = secondary electrons

SEM = Scanning electron microscopy

TEM = Transmission electron microscopy

TEOS = Tetraethylorthosilcate

TTIP = Titanium tetraisopropoxide

UV = ultraviolet

VB = valence band

VOC = volatile organic compound

XRD = X-ray powder diffraction

$\Delta G^0$  = Gibbs free energy

# Content

<b>1</b>	<b>INTRODUCTION.....</b>	<b>8</b>
<b>2</b>	<b>THEORY.....</b>	<b>9</b>
<b>2.1</b>	<b>PHOTOCATALYSTS.....</b>	<b>10</b>
<b>2.2</b>	<b>SYNTHESIS OF NANOSIZED TIO<sub>2</sub>.....</b>	<b>16</b>
<b>2.3</b>	<b>DIP-COATING.....</b>	<b>20</b>
<b>2.4</b>	<b>CHARACTERIZATION METHODS .....</b>	<b>21</b>
<b>3</b>	<b>EXPERIMENTAL.....</b>	<b>23</b>
<b>3.1</b>	<b>SYNTHESIS OF TIO<sub>2</sub> NANOPARTICLES .....</b>	<b>23</b>
<b>3.1.1</b>	<b>PREPRATION OF TIO<sub>2</sub> PARTICLES .....</b>	<b>24</b>
<b>3.1.2</b>	<b>PREPARATION OF SILVER DOPED TIO<sub>2</sub> PARTICLES .....</b>	<b>25</b>
<b>3.2</b>	<b>SYNTHESIS OF FILMS.....</b>	<b>26</b>
<b>3.2.1</b>	<b>PREPARATION OF SIO<sub>2</sub> SOLS.....</b>	<b>26</b>
<b>3.2.2</b>	<b>PREPARATION OF TIO<sub>2</sub> SOLS.....</b>	<b>29</b>
<b>3.2.3</b>	<b>DIP COATING PROCESS .....</b>	<b>29</b>
<b>3.3</b>	<b>CHARACTERIZATION.....</b>	<b>31</b>
<b>3.3.1</b>	<b>THE X-RAY POWDER DIFFRACTION.....</b>	<b>31</b>
<b>3.3.2</b>	<b>SCANNING ELECTRON MICROSCOPY.....</b>	<b>33</b>
<b>3.3.3</b>	<b>ATOMIC FORCE MICROSCOPY.....</b>	<b>35</b>
<b>3.3.4</b>	<b>RAMAN CONFOCAL MICROSCOPY .....</b>	<b>36</b>

<b>3.3.5</b>	<b>OPTICAL EMISSION GLOW DISCHARGE SPECTROSCOPY .....</b>	<b>37</b>
<b>3.3.6</b>	<b>PHOTODEGRADATION ACTIVITY MEASUREMENT .....</b>	<b>38</b>
<b>4</b>	<b>CONCLUSION.....</b>	<b>41</b>
<b>5</b>	<b>ACKNOWLEDGMENTS .....</b>	<b>41</b>
<b>6</b>	<b>LITERATURE.....</b>	<b>42</b>

# 1 Introduction

Titanium dioxide ( $\text{TiO}_2$ ) belongs to important compounds produced by chemical industry and finds number of applications comprising its utilization in paint industry (interior and exterior paints), as a food additive (e.g. in milk), in cosmetics (sunscreen), pharmacy (coating of pills) and many others [1,2]. These applications are related to the  $\text{TiO}_2$  manufactured by the common methods, most often by sulfate and chloride process. The final product of these methods is  $\text{TiO}_2$  in form of rutile with the crystallite size in the order of hundreds nanometers and this size range corresponds to real particle size also [2].

By the decreasing of  $\text{TiO}_2$  crystallite size the active surface area significantly increases and the frequency of electron-hole pair generation also dramatically grows, whereas the electron-hole generation is responsible for photoactive properties of  $\text{TiO}_2$ . Photoactivity of the nanosized  $\text{TiO}_2$  enlarges its utilization to the other industrial areas like energetic, processes related to the degradation of environmental pollutants.

The photoactivity of the pure  $\text{TiO}_2$  is induced by the absorption of photon with energy higher than 3.2 eV (band gap energy  $E_g$  of  $\text{TiO}_2$ ). This energy can be supplied by electromagnetic irradiation with wavelengths shorter than 384 nm, though the photons with sufficient energy represent only 5 % of sunlight. For the more effective utilization of sunlight the modification of  $\text{TiO}_2$  structure is desired. The most often utilized modification comprises dopation by other elements, namely by the nitrogen, another method is for example based on the sensitization of  $\text{TiO}_2$  surface by organic dyes [2].

Although the nanosized  $\text{TiO}_2$  is excellent photocatalyst, the possible environmental risks related to its nanodimension should not be omitted [3]. One possible way how to prevent these possible risks is preparation of the photocatalytic materials in the form of thin layers captured on the selected substrates [4].

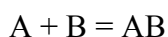
The aim of this work is preparation and characterization of photocatalytic material based on titanium dioxide  $\text{TiO}_2$  in form of powder and film.



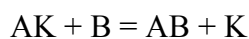
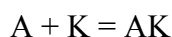
## 2 Theory

Catalysts are used in many industrially and biochemically important reactions and development of new catalysts is one of the major fields in chemistry. Using the catalysts the rate of chemical reactions can be altered because the alternative (catalyzed) route has lower activation energy than the uncatalyzed one. The catalyst is able to greatly alter the reaction rate even if used in small amount and is not consumed during the reaction. Catalyst may participate in several chemical transformations as can be seen from the comparison of uncatalyzed and catalyzed reaction below.

Uncatalyzed reaction:



Catalyzed reaction:



The catalyst provides an alternative reaction pathway with the same reaction product at the end. Energetic diagram of uncatalyzed and catalyzed reaction is shown in Fig. 1.

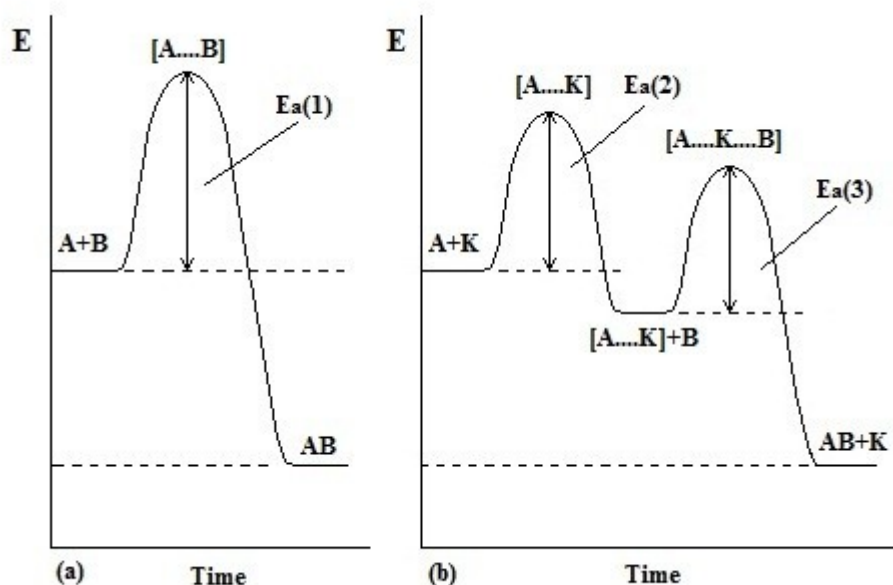


Fig. 1 Energetic diagram of uncatalyzed reaction a) and catalyzed reaction b), where  $E_a$  is activation energy. Picture taken from [5].

The activation energy  $E_a(1)$  of uncatalyzed reaction is higher than activation energy of catalyzed reaction  $E_a(2)$  or  $E_a(3)$ .

With respect to the reaction environment the catalytic reactions are divided into two groups:

1. Homogeneous catalysis - catalyst and the reactants occur in the same phase i.e. gas or liquid. For homogeneous catalysis is typical that the reactants reacts at first with catalysts and transition compounds are created.
2. Heterogeneous catalysis - in heterogeneous catalysis, the catalyst is in different phase (typically solid) than other reactants (typically liquid or gas). For heterogeneous catalysis is typical that the transition compounds are adsorbed on the surface of catalyst.

The catalysts can be divided by their effect on reaction rate:

1. The catalysts that increase the reaction rate (speed the reaction) are called positive catalysts.
2. The catalysts that decreases reaction rate (slows the reaction) are called negative catalysts or inhibitors.

The effect of catalysts on reaction rate can be further amplified by promoters or stopped by catalytic poisons [5].

## 2.1 Photocatalysts

Photocatalysts are generally semiconductors, where the transition of electron from valence band (VB) to conductive band (CB) is caused by its photoexcitation by the photon with energy higher than the energy of band gap ( $E_g$ ).  $E_g$  is an energy range in a solid where no electron states can exist. The  $E_g$  is situated between valence band (VB) and conductive band (CB) as shown in Fig. 2.

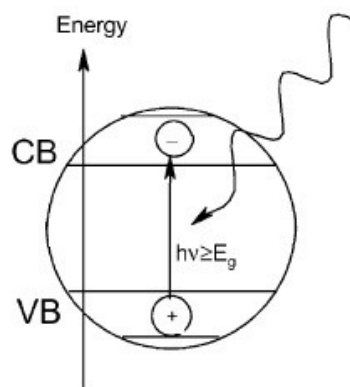


Fig. 2 In semiconductor the band gap separates valence band VB and conductive band CB, picture modified from [2].

The ability of semiconductor to transfer photoinduced electron to an adsorbed particle is determined by the band energy positions of the semiconductor and the redox potential of adsorbed compounds.

The energy level at the bottom of conduction band corresponds to reduction potential of photoinduced electrons. The energy level at the top of valence band corresponds to the oxidation ability of photoinduced holes. Both these values determines the reduction and oxidation ability of the system [2]. The band positions: top of valence band and bottom of conductive band of several semiconductors, and selected redox potentials are schematically shown in Fig. 3.

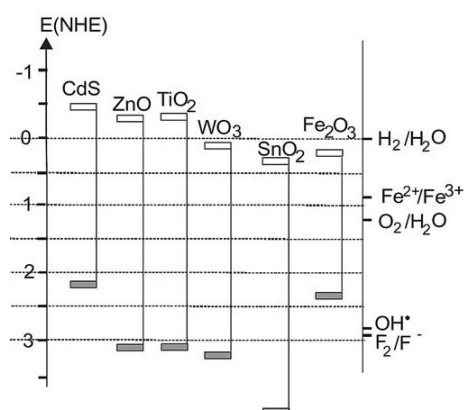


Fig. 3 The band positions of several semiconductors together with chosen redox potentials. Where E(NHE) is energy of normal hydrogen electrode, darker rectangles represents the top of valence band, the lighter rectangles represents the bottom of conductive band, modified from [2].

The lack of continuum of interband states of semiconductors in comparison with metals, prolongs the recombination time of electron-hole pair. Longer recombination time enables diffusion of electrons and holes to catalyst's surface and initiate redox reaction [2].

*Photoduced reactions on a semiconductor particle*

The electron-hole pair is generated after absorption of photon with sufficient energy. The generated electron-hole pair is responsible for oxidation and reduction reactions that take place on the surface of the semiconductor particle. The oxidation and reduction reactions together with electron-hole recombination takes place at the same time, but with different reaction speeds. [2]. The scheme of phototinduced reactions on the semiconductor particle is shown in Fig. 4.

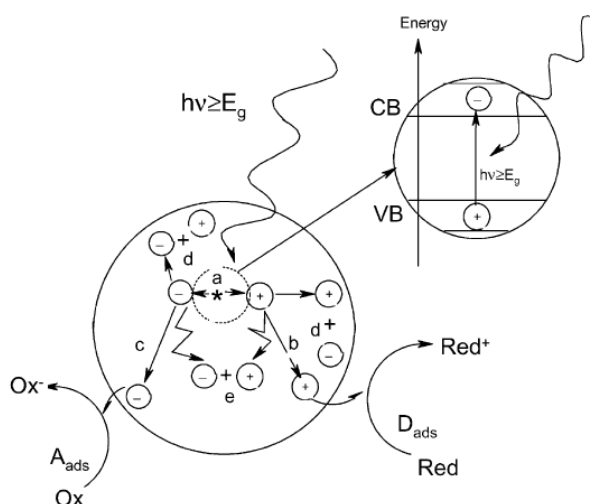


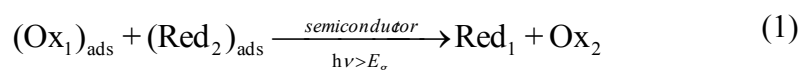
Fig. 4 Scheme of photoinduced reactions on the semiconductor particle. A- Acceptor, D-donor, <sub>ads</sub>- adsorbed,  $h\nu$  - photon energy,  $E_g$ - band gap energy, a) generation of electron-hole pair, b) oxidation reaction, c) reduction reaction, d) surface electron –hole recombination, e) bulk electron-hole recombination. Picture taken from [2].

The photoinduced reactions shown in Fig. 4 corresponding to the reactions on the surface of TiO<sub>2</sub> particle are most often expressed by following scheme:

- a)  $\text{TiO}_2 + h\nu \rightarrow \text{TiO}_2(e^- + h^+)$  generation of electron/hole pair
  - b)  $e^- + \text{M}^{n+} \rightarrow \text{M}^{(n-1)+}$  reduction reaction of metal cation [2].  
or  $e^- + \text{O}_2(\text{ads}) \rightarrow \text{O}_2^{\bullet-}$  oxygen radical generation from adsorbed O<sub>2</sub> [4].
  - c)  $h^+ + \text{H}_2\text{O} \rightarrow \text{HO}\bullet + \text{H}^+$  oxidation of adsorbed water
- (hν - photon energy, M<sup>n+</sup> - metal ion, h<sup>+</sup> - hole, e<sup>-</sup> - electron)

#### *Photosynthesis vs. photodegradation*

The scheme of photocatalyzed reaction (1) is shown below:



In most photosynthesis reactions involving TiO<sub>2</sub>, ΔG<sup>0</sup> is negative (ΔG<sup>0</sup> < 0) and the reactions are photocatalytic rather than photosynthetic [2].

Almost every functional group with non bonded electron pair or with π-conjugation is prone to oxidation by TiO<sub>2</sub>. Reductive transformation of organic compound is possible under certain experimental conditions (oxygen absence and proton source) [2]. The reductive transformation is usually less efficient than the oxidative one. There are two reason for that:

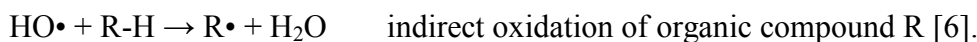
1. The reducing power of a conduction band electron is significantly lower than the oxidizing power of a valence band hole.
2. Most reducible substrates cannot kinetically compete with oxygen in trapping photogenerated conduction band electrons [2].

Due to these reasons the main research focus is on the photodegradation of compounds rather than their photosynthesis.

#### *Photodegradation of organic compound*

As mentioned above, the reductive transformation of organic compounds is usually less efficient than the oxidative one. The photodegradation of organic compound proceeds by its direct oxidation by hole h<sup>+</sup> and indirect oxidation by hydroxyl radical HO•.

The photodegradation of the organic compound proceeds according to these reactions:



Where R is organic compound. The photodegradation of organic compound can indirectly proceed by other activated oxygen species e.g.  $O_2^-$ ,  $HOO^-$ ,  $HOOH$ ,  $HOO\cdot$ ,  $HO\cdot$ , depending on reaction conditions. The organic compounds can be degraded to basic inorganic compounds: water, carbon dioxide and mineral acid [2].

#### *Parameters affecting photodegradation process*

The parameters like photocatalyst dosage, UV light intensity, concentration and nature of pollutant, temperature, oxygen concentration, pH, humidity for photodegradations in gaseous phases and others significantly affects photodegradation rate.

Below are analyzed several factors influencing the photodegradation process:

Dosage - With higher dosage of the photocatalyst the total surface area grows and therefore more active sites are available.

UV light intensity - The reaction order is dependent on the intensity of used light. The borderline intensity is  $25 \text{ mW/cm}^2$ . The first order regime is for intensities up to  $25 \text{ mW/cm}^2$ , half order regime is for intensities above the  $25 \text{ mW/cm}^2$  borderline.

Concentration and nature of pollutant - The photocatalyst has limited amount of active sites and in the situation of excess amount of pollutant is saturated and the photocatalytic activity has constant rate.

Temperature -The photocatalytic oxidation is not much affected with minor temperature changes (the energy to excite electron from the valence band is greater than the thermal energy). However the temperature affects desorption time of the pollutant, with higher temperature the desorption time is shorter.

Oxygen concentration - The dissolved molecular oxygen is electrophilic and reduces electron hole recombination. However at high concentration of the oxygen the surface of  $TiO_2$  becomes intensively hydroxylated by OH groups which inhibits the adsorption of pollutant.

pH- The pH affects the surface charge of the  $TiO_2$ , hydrophobicity,  $HO\cdot$  production, adsorption of pollutant etc.

Humidity for photodegradations in gaseous phases - The water plays important part in constant production of hydroxyl radicals needed for catalytic activity, as can be seen in above mentioned reaction c)  $h^+ + H_2O \rightarrow HO\cdot + H^+$  [2].

#### *TiO<sub>2</sub> as a photocatalyst*

In 1972 A. Fujishima and K. Honda published article about ultraviolet (UV) light splitting of water using TiO<sub>2</sub> photoanode and platinum (Pt) counter electrode. This article showed hidden possibilities of this material and brought attention to the photocatalytical materials based on TiO<sub>2</sub>.

TiO<sub>2</sub> crystallizes in three forms : anatase, rutile and brookite and their crystal structures are shown in Fig. 5

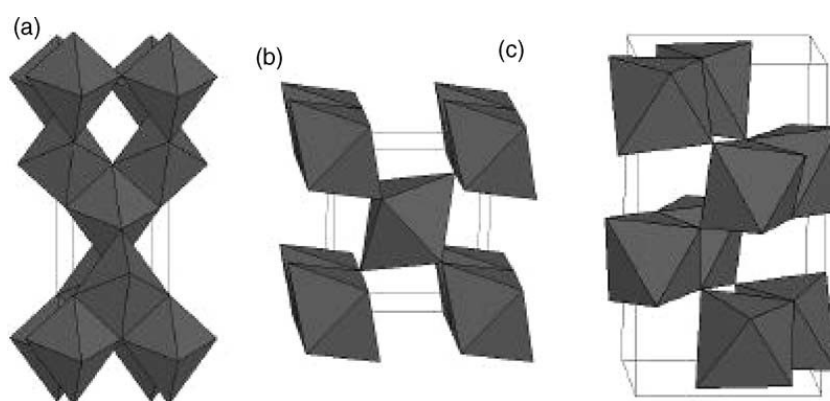


Fig. 5 The crystal structure of TiO<sub>2</sub> forms: anatase (a), rutile (b), brookite (c). Picture taken from [2].

The anatase is most thermodynamically stable at sizes less than 11 nm, brookite is thermodynamically stable at sizes between 11 and 35 nm and rutile is most thermodynamically stable at sizes greater than 35 nm. At the room temperature the anatase in the bulk form is stable but at temperatures higher than 600°C transforms to rutile. For nanosized TiO<sub>2</sub> the transformation temperature from anatase to rutil is lower [2].

TiO<sub>2</sub> is a transition metal oxide and due to the oxygen vacancies is TiO<sub>2</sub> an n-type semiconductor (has an excess of negative (n-type) electron charge carriers) [2]. The TiO<sub>2</sub> band gap energy is different for each of the three forms, anatase and brookite has  $E_g = 3.20$  eV, whereas rutile has  $E_g = 3.02$  eV. TiO<sub>2</sub> in anatase form shows the highest photocatalytic activity as was shown in number of publications e.g [2]. Anatase can be excited

by light with wavelength shorter than 384 nm. The photocatalytic activity of TiO<sub>2</sub> can be further enhanced by several methods such as dopation, thermal treatment, etc [2].

Dopation-doping of TiO<sub>2</sub> photocatalyst with various elements may enhance its photocatalytic properties. The dopation modifies:

- light absorbtion capability of TiO<sub>2</sub>
- absorbtion capacity of the substrate at the surface of catalyst
- interfacial charge transfer

Thermal treatment- TiO<sub>2</sub> is clacined and the anatase rutile transformation takes place.

## 2.2 Synthesis of nanosized TiO<sub>2</sub>

*Short owerview of methods for preparation of nanosized TiO<sub>2</sub>*

Nanosized TiO<sub>2</sub> can be prepared by the sol-gel method, solvothermal methods, microemulsion methods, combustion synthesis, electrochemical synthesis, chemical vapour deposition (CVD), physical vapour deposition (PVD), spray pyrolysis deposition (SPD), etc. The principle of above mentioned methods is shortly described below [2].

Solvothermal methods – The chemical reactions proceeds in aqueous or organic media under self produced pressure at low temperatures.

Microemulsion methods – Microemulsions of water in oil serve as reaction media.

Combustion synthesis – The solution or compound with redox mixture is rapidly heated.

Electrochemical synthesis – In acidic, oxygen free media are electrodeposited TiO<sub>2</sub> films from titanium inorganic salts.

Chemical vapour deposition – Decomposed precursors or chemically prepared compounds are formed in gas phase and coated on surface of the substrate.

Physical vapour deposition – Substances stable in gas phase are coated on surface of the substrate. There is no transformation from precursor to product.



Spray pyrolysis deposition – Aerosol formed from the precursor solution is coated on surface of the substrate.

*Sol-gel method*

The sol-gel method represents an easy method for synthesizing TiO<sub>2</sub> materials. Purity, homogeneity, easy dopation of the sol, ability to coat large areas etc. belongs to the advantages of the sol-gel methods.

Sol-gel methods can be distinguished by the nature of precursors. There are two types of precursors:

The non-alkoxide precursors [2] are inorganic salts e.g. nitrates, chlorides, acetates, carbonates, etc. This method requires additional retrieving of the inorganic anion.

The alkoxide precursors are metal alkoxides with general formula Ti(OR)<sub>4</sub> [2]. Titanium alkoxides used as titanium precursors are shown in Fig. 6 – Fig. 8.

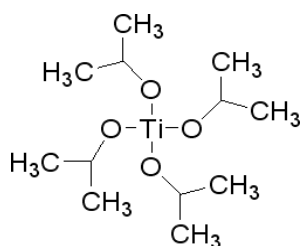


Fig. 6 Titanium tetraisopropoxide

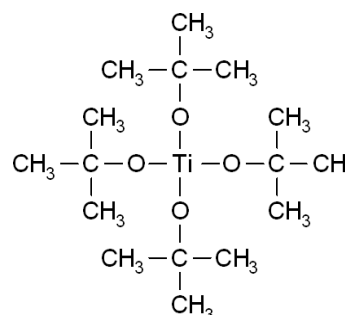


Fig. 7 Titanium tetra-tert-butoxide

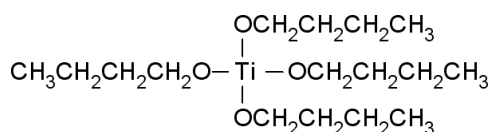
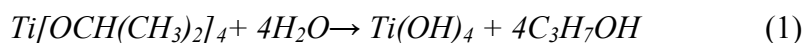


Fig. 8 Titanium tetrabutoxide

In the alkoxide method the TiO<sub>2</sub> is formed in sol or gel or precipitated by hydrolysis and condensation of titanium alkoxides. The equation describing the hydrolysis of the titanium tetraisopropoxide (TTIP) is shown in the following reaction scheme (1):



For better control over microstructure forming it is necessary to separate and modify the hydrolysis and condensation steps [2]. There are several ways how to achieve the modification. Below are some of them described.

#### *Alkoxide modification*

Alkoxide modification by complexation with coordination agents (e.g. carboxylates or β-diketonates) that hydrolyze slower than alkoxide ligands [2].

#### *Acid-based catalysis*

Acid- based catalysis enables separation of hydrolysis from condensation steps. Acid catalysis increases hydrolysis rate and completely crystalline powders are obtained from fully hydrolyzed precursors [2].

#### *Base- catalysis*

Base-catalysis promotes condensation and amorphous powders containing unhydrolyzed alkoxide ligands are obtained [2].

#### *Other treatments affecting the final microstructure of TiO<sub>2</sub>*

Thermal treatment - Calcination at temperatures 400-600°C in order to crystallize rutile and anatase and to remove an organic part. The calcination leads to phase transformation, the decrease of surface area (due to crystallite growth) and loss of surface hydroxyl groups [2].

Washing – The washing is a cleaning process where the particle surface is washed with a solvent. The solvent can affect chemical composition, crystallization and surface charge [2].

Dopation – The dopation is a popular method for producing homogenous phase multicomponent oxides mixed at molecular level. Elements used for dopation comprise e.g. N, S, Ca, Cu, Fe, Pt, Ag, Au, La etc [2].

Templating - Ionic and neutral surfactants as well as block polymers are employed as templates to prepare mesoporous TiO<sub>2</sub> (a mesoporous material has pore diameter between 2-50 nm) [2].

Hydrothermal treatment – The hydrothermal treatment employs the combination of heat and water as a media to convert the sample. The sol-gel method coupled with the hydrothermal treatment leads to formation of mesoporous structures even after the heating at 500°C [2].

Autoclaving- During autoclaving is the sample treated at high temperatures and pressures. Autoclaving of the sol allows controlled growth of particles and leads to product with homogenous particle distribution [2].

## 2.3 Dip-coating

The dip-coating is a very popular method for the coating of substrates by sol prepared by sol-gel methods. The principle of the method is to dip the substrate material into the coating solution and withdraw it out, whereas the whole process proceeds under regulated conditions. During one cycle the substrate material is dipped one time and withdrawn out, the cycle can be repeated.

Using the dip coating method a uniform thin films can be obtained. Another advantage of the dip-coating method is the size of the samples, it is possible to coat large areas and various shapes of the substrate material. Multi layer coating enables production of the films with varying optical characteristics. The dip-coating has complex dependency on various parameters such as: concentration of the solution, its viscosity, angle and speed of withdrawal, surface tension of solution, vapor pressure and relative humidity above the sol [7].

Several factors influencing the dip-coating process are summarized below:

- The coating thickness increases with withdrawal speed.
- The angle of withdrawal is commonly  $90^\circ$  with respect to the solution surface, any divergence from this angle means that the coating thickness would not be same on both sides of the substrate.
- Good wetting of the substrate material is a very important factor, for this reason ethanol is most commonly used as a solvent.
- The water can be added to the coating sol, depending on the hydrolysis rate. Prehydrolyzed and precondensed solutions are acquired by this procedure. The prepared solution has limited life time, because the reaction continually proceeds and thus the stability of the sol is limited.
- By controlling the water vapor content in the atmosphere during the coating process is possible to keep the hydrolysis processes even in the already deposited layer. The polycondensation process takes place at the same time as hydrolysis process until the thermal treatment begins.

## 2.4 Characterization methods

Basic integrated characterization of the prepared TiO<sub>2</sub> sample can be generally divided into four stages: chemical analysis, phase analysis, determination of the sample morphology and testing of application features. Below are shown chosen characterization methods for each stage.

The chemical analysis provides information about the elemental composition and enables to perform theoretical assessment of the compounds presented in the sample. According to the nature of the sample it is possible to divide them into analysis on “dry way” and “wet way”.

The “dry way”- The samples that are going to be analyzed are in solid or powder form and the most often utilized method is X-ray fluorescence spectrometry (XRFS). The samples for this method have to be compressed into pellets, or prepared in the form of borate pearls.

For the “wet way” methods the sample has to be transferred into solution. The sample can be decomposed in suitable solvent (water, acids, bases) or prepared by melting procedure. The instrumental methods for analysis of the prepared samples are represented by:

- Optical emission spectrometry with inductively coupled plasma (ICP-OES) - used for analysis of trace elements.
- Atomic absorption spectroscopy (AAS) – is used for determining the concentration of a particular element in the sample.

The other methods are represented by:

- Elemental analysis – enables precise quantitative analysis of C, H, N, O, S elements. The sample is incinerated and exhaust gases are investigated for the above mentioned elements.
- Infrared spectroscopy - provides information about the presence of the chemical bonds in compounds forming the sample.
- Raman spectroscopy - provides information about the vibrational states related to a characteristic chemical bonds and the symmetry of molecules.

The phase analysis is determined using an X-ray diffraction techniques (XRD). This method is suitable mainly for the crystalline materials. The crystallite size and stress can be also determined from the registered XRD patterns.

Morphology is examined by:

- Scanning electron microscopy (SEM) - provides information about the size and shape of particles. Non-conductive samples have to be covered with a Au/Pd film.
- Transmission electron microscopy (TEM) - provides the information about size and shape of particles and films. The TEM is suitable for examination of thin samples.
- Atomic force microscopy (AFM) - provides the information about the surface topography of the studied samples.

Testing of application features e.g. the photoactivity of the  $\text{TiO}_2$  in liquid phase is often evaluated by photodegradation of organic dyes [8] which represent the common contaminant of water coming from the textile industry. The photoactivity of the  $\text{TiO}_2$  in gaseous phase is often evaluated by photodegradation of nitrogen oxides ( $\text{NO}_x$ ) [9] or volatile organic compounds (VOCs) – e.g. toluene [10]. The procedure of photodegradation of  $\text{NO}_x$  and VOCs is described by ISO standards [11, 12].

### **3 Experimental**

The experimental part was focused on the preparation of photocatalytically active TiO<sub>2</sub> in the form of fine powder consisting of a TiO<sub>2</sub> nanoparticles and on the preparation of TiO<sub>2</sub> thin films. XRD method, Scanning electron microscopy, Raman microscopy, Optical emission glow discharge spectrometry (OE GDS) and Atomic force microscopy were used for the characterization of the prepared samples. Photodegradation activity was evaluated by the photodegradation of organic model dye - acid orange 7.

Experimental part is divided into two parts:

1. Synthesis of TiO<sub>2</sub> nanoparticles and TiO<sub>2</sub> thin films.
2. Characterization of the prepared samples.

#### **3.1 Synthesis of TiO<sub>2</sub> nanoparticles**

The synthesis of the TiO<sub>2</sub> particles was performed according to the modified procedure described by Lee et al. [13]. Generally this method is based on the precipitation of TiO<sub>2</sub> nanoparticles from the solution of titanium tetraisopropoxide and water. TiO<sub>2</sub> nanoparticles and silver doped TiO<sub>2</sub> nanoparticles were prepared by this procedure.

### 3.1.1 Preparation of TiO<sub>2</sub> particles

In the first step the solution of 0.2500 g of sodium citrate tribasic dihydrate p.a. (Lachema) in 250 ml of distilled water was prepared and heated up to 80 °C. Subsequently 48.25 g of TTIP (Sigma Aldrich) and 5 ml of concentrated HNO<sub>3</sub> (Mach chemicals) were added to the prepared citrate solution. The resulting white slurry was vigorously stirred using electromagnetic stirrer. The temperature was lowered to 50 °C and the mixture was left to age for 24 hours with permanent stirring. The prepared white gel was dried at ambient temperature, powderized in agate mortar and assigned as sample TiO<sub>2</sub>. The method is schematically described in Fig.9, the apparatus used for the synthesis is shown in Fig.10. The samples were also calcined at 300 and 400 °C for 1 hour, the samples were assigned as TiO<sub>2</sub>-300 and TiO<sub>2</sub>-400, respectively.

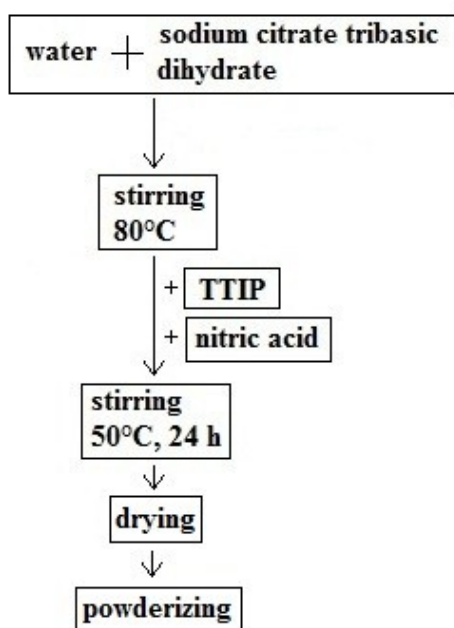


Fig.9 The synthesis scheme of the TiO<sub>2</sub> nanoparticles.



Fig.10 The synthesis apparatus of nanoparticles.



### 3.1.2 Preparation of silver doped TiO<sub>2</sub> particles

The preparation of silver doped sample is closely similar to the preparation of the TiO<sub>2</sub> particles, the only difference is in composition of the initial citrate solution which is enriched with silver by dissolution of 0.0860 g of silver nitrate (Lachema). This amount of silver nitrate gives theoretically 0.21 wt.% of Ag in resulting sample assigned as Ag-TiO<sub>2</sub>. The method is schematically described in Fig. 11.

The samples were also calcined at 300 and 400 °C for 1 hour and were assigned as Ag-TiO<sub>2</sub>-300 and Ag-TiO<sub>2</sub>-400, respectively.

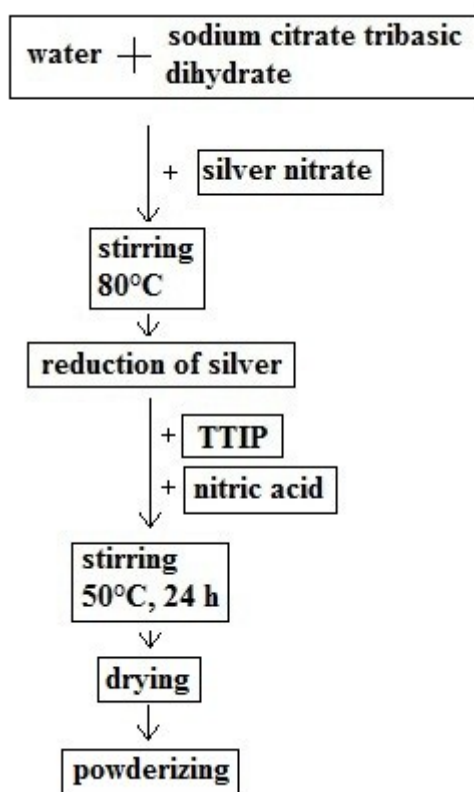


Fig. 11 The scheme of the synthesis of Ag-TiO<sub>2</sub> nanoparticles.

## 3.2 Synthesis of films

The TiO<sub>2</sub> thin films were deposited using dip-coating method and the glass tubes and plates were used as a substrate. The TiO<sub>2</sub> thin films were deposited directly on the surface of the glass sheets and tubes and also, with respect to several literature recommendations e.g. [14], on glass substrates precoated by SiO<sub>2</sub> thin layer. The SiO<sub>2</sub> coating was used to standardize the morphology and chemical composition of the surface layer of the substrate. The glass plates were used as a substrate for their eligibleness for surface characterization using AFM and Raman microscopy, the glass tubes were coated with respect to newly developed method for testing of the photodegradation activity.

### 3.2.1 Preparation of SiO<sub>2</sub> sols

For the reasons explained later there were prepared two different SiO<sub>2</sub> sols assigned as SiO<sub>2</sub>-A, resp. SiO<sub>2</sub>-B.

#### *The synthesis of the SiO<sub>2</sub>-A film*

The synthesis of the SiO<sub>2</sub>-A film was performed according to the procedure described by Huang et al. [15]. The sol used for SiO<sub>2</sub> coating was prepared by mixing of 134 ml of ethanol p.a. (Lachner) with 51 ml of TEOS (Tetraethylorthosilcate) synthesis grade (Sigma Aldrich) and 14.5 ml of distilled water. Then 0.4 ml of concentrated HCl (Mach chemicals) was added as a catalyst. The obtained solution was heated for 90 minutes at 70 °C (the temperature was measured in the water bath) under the reflux and vigorous stirring using electromagnetic stirrer. After the heating the solution was cooled in water bath for 30 minutes. After the cooling 2.5 ml of 0.5M NH<sub>4</sub>OH p.a. (Lachner) was dropwise added to the cooled solution. The solution was stirred all the time through the synthesis. The prepared gel was dip-coated on glass slides and tubes. The synthesis scheme is shown in Fig.12, the apparatus used for the SiO<sub>2</sub>-A sol preparation is depicted in Fig.13.

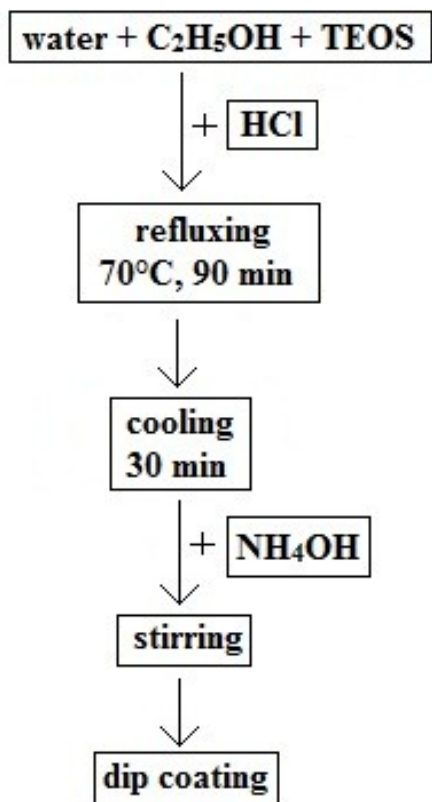


Fig.12 The synthesis scheme of SiO<sub>2</sub>-A film.



Fig.13 The synthesis apparatus of SiO<sub>2</sub>-A sol.

### *The synthesis of the SiO<sub>2</sub>-B film*

The synthesis of the SiO<sub>2</sub>-B film was performed according to the modified procedure described by Zita et al. [14]. The SiO<sub>2</sub> sol for dip-coating was prepared by mixing of the 75 ml of ethanol p.a. (Lachner) with 50 g of TEOS p.a. (Sigma Aldrich) under vigorous stirring for 10 minutes. After this time period 12.5 ml of distilled water and 2.5 ml of concentrated HNO<sub>3</sub> (Lachner) were added. The solution was then stirred for 60 minutes. Synthesis scheme is shown in Fig.14. . The synthesis aparature of SiO<sub>2</sub>-B sol looks similar to the one in Fig.10.

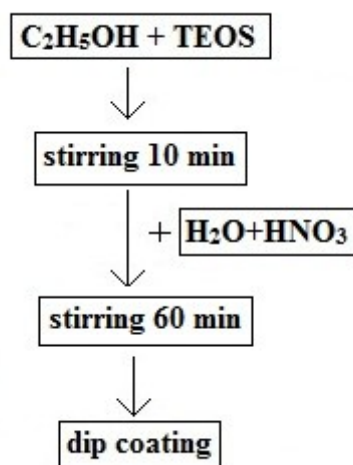


Fig.14 The scheme of the synthesis of SiO<sub>2</sub>-B film.

### 3.2.2 Preparation of TiO<sub>2</sub> sols

The synthesis of the TiO<sub>2</sub> films was performed according to the procedure described by Addamo et al. [4]. The TiO<sub>2</sub> sol used for dip-coating was prepared by mixing of 400 ml of distilled water and 3.8 ml of concentrated HNO<sub>3</sub> (Mach chemicals), and then 34.8 g of TTIP p.a. (Sigma Aldrich) was dropwise added. The mixture was then stirred for 20 hours using electromagnetic stirrer. After this period the sol was heated up to 50 °C and stirred for 2 hours at this temperature. The prepared sol was dip-coated on the original and SiO<sub>2</sub> pre-coated glass slides and tubes. The synthesis scheme is shown in Fig.15. The apparatus used for the TiO<sub>2</sub> sol preparation looks similar to the one in the Fig.10.

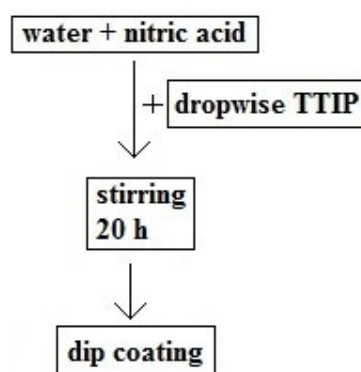


Fig.15 Schema of synthesis of TiO<sub>2</sub> film.

### 3.2.3 Dip coating process

The glass tubes and slides were dip coated using COATER5 (idLAB). The glass tubes and slides were thoroughly cleaned before the coating. The cleaning process consisted of washing the tubes and plates in order of precedence with: tap water mixed with detergent, tap water, distilled water and finally washed with ethanol. The cleaned tubes and plates were dried at 100 °C for 15 minutes. The coating parameters were: dipping speed 20 cm/min, the delay 3s and withdrawing speed 6 cm/min. The obtained samples were dried at ambient temperature and then dried at 100 °C for 1 hour.

At first the pre-coating of glass substrates by  $\text{SiO}_2$  thin layer was performed. The pre-coated substrates were dip-coated with  $\text{TiO}_2$  sol. After analyzing of the first  $\text{TiO}_2$  film samples by OE GDS it was discovered that the  $\text{SiO}_2$  layer prevents deposition of the  $\text{TiO}_2$  layer. Although two different sols of  $\text{SiO}_2$  were used for pre-coating of the glass plates and tubes, both showed hydrophobic effect and the deposition of  $\text{TiO}_2$  was impossible. With respect to this result the  $\text{SiO}_2$  pre-coating was abandoned and  $\text{TiO}_2$  sol was coated only on bare glass substrate.

In the case of  $\text{TiO}_2$  sol it was observed that one layer (the layer acquired after one dip-coating cycle) is sufficient to equally cover the substrate glass tube or plate, and the repeated dip-coating procedures were tested only with the aim to describe the effect of the number of the dip-coating cycles on the relative thickness of the  $\text{TiO}_2$  layers. There were prepared glass plates covered with 1, 2 and 3 layers of  $\text{TiO}_2$ . After the coating of each layer the samples were dried at  $100\text{ }^\circ\text{C}$  for 1 hour and calcined at  $500\text{ }^\circ\text{C}$  for 1 hour.

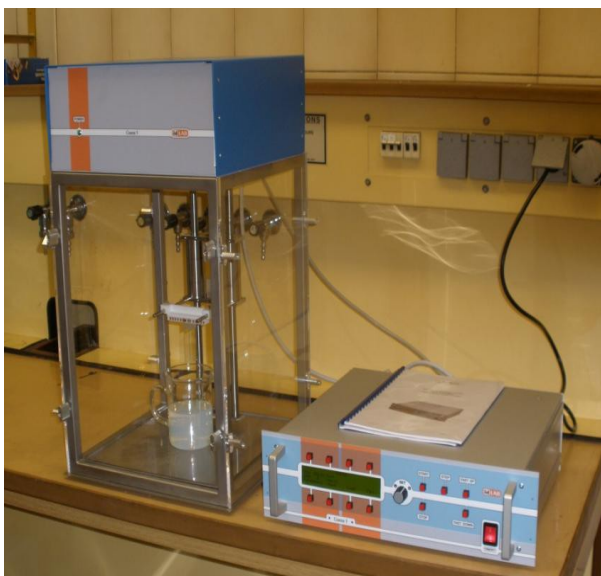


Fig.16 The dip coater.



Fig.17 The dip coating of glass plate into the  $\text{SiO}_2$ -B sol.

## 3.3 Characterization

The characterization methods were chosen in order to confirm the presence of TiO<sub>2</sub>, to determine anatase/rutile phase ratio, to measure the photocatalytic activity and to determine the effect of thermal treatment on the prepared samples. The chosen characterization methods are commonly used for these materials (photocatalytic nanoparticles and films respectively) according to appropriate literature [2, 4, 13].

### 3.3.1 The X-ray powder diffraction

The XRD patterns were gathered using Bruker D8 Advance diffractometer (Bruker AXS, Germany) with fast position sensitive detector VÅNTEC 1. The source of X-ray irradiation was cobalt tube (CoK $\alpha$ ,  $\lambda = 1.7889\text{\AA}$ ). The powder samples were pressed in rotational holder and measured in reflection mode. The XRD patterns were evaluated using the database PDF 2 Release 2004 (International Centre for Diffraction Data). The XRD patterns of the prepared powdered samples are shown in Fig.18 and Fig.19. The dried samples (TiO<sub>2</sub> and Ag-TiO<sub>2</sub>) are composed only of the anatase and rutile, no impurities in the samples were found. The heat treated samples consists of anatase and rutile. The average size ( $L_c$ ) of anatase crystallite was calculated using equation (1) proposed by Scherrer [16].

$$L_c = \frac{K \times \lambda}{FWHM \times \cos \theta} \quad (1)$$

Where K is shape factor (for TiO<sub>2</sub> nanoparticles the K = 0.89),  $\lambda$  is the X ray wave length (in case of CoK $\alpha$  irradiation –  $\lambda = 0.17889$  nm),  $\theta$  is Bragg angle in radians, FWHM stands for full width at half maximum of the peak. The anatase crystallite size ( $L_c$ ) calculated for the prepared powder samples is shown in Tab. 1.

Tab. 1 The anatase crystallite size Lc (nm)

sample	Lc	sample	Lc
TiO <sub>2</sub>	4	Ag-TiO <sub>2</sub>	4
TiO <sub>2</sub> -300	6	Ag-TiO <sub>2</sub> -300	6
TiO <sub>2</sub> -400	7	Ag-TiO <sub>2</sub> -400	7

From the comparison of the calculated anatase crystallite size values (Tab. 1) is apparent that Ag dopation has no effect on the crystallite size and that crystallite size increases with the calcination temperature.

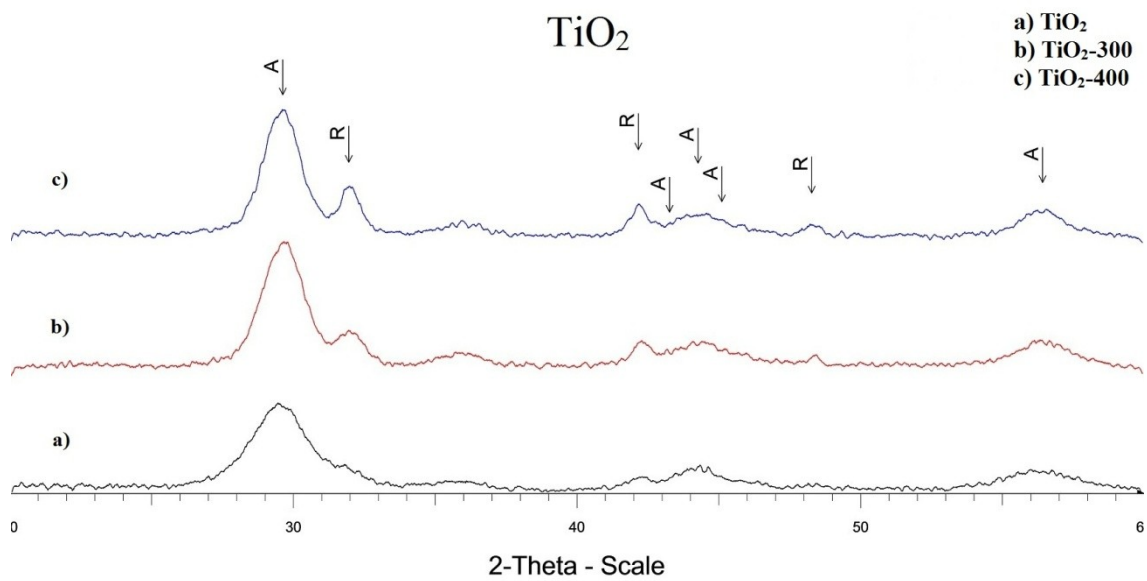


Fig.18 XRD patterns of TiO<sub>2</sub> nanoparticles, where A is anatase and R rutile.

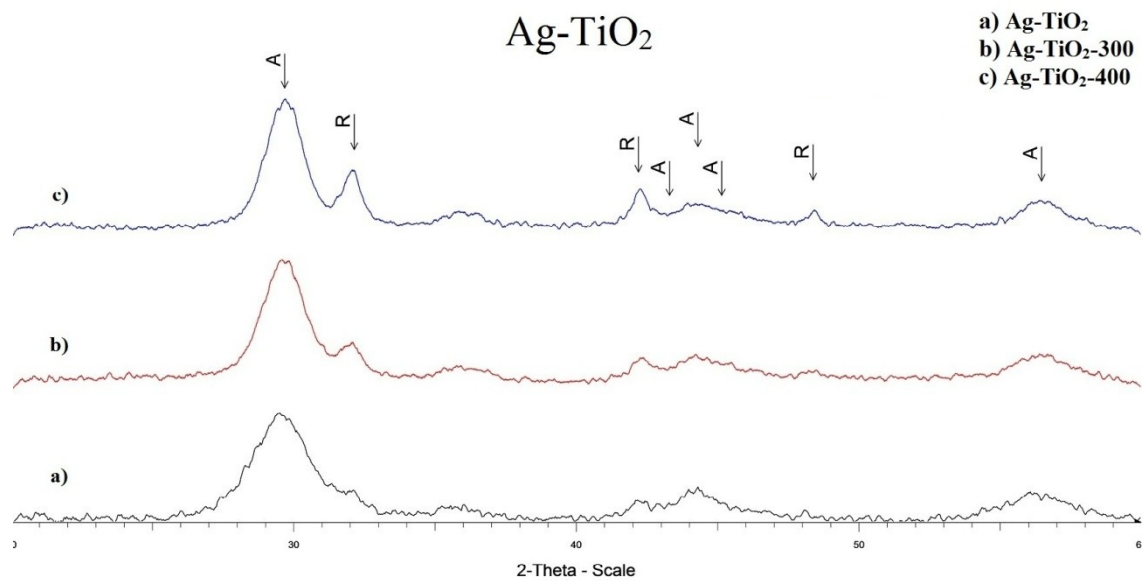


Fig.19 XRD patterns of Ag-TiO<sub>2</sub> nanoparticles, where A is anatase and R rutile.



From the comparison of the diffraction patterns of undoped and Ag doped TiO<sub>2</sub> (Fig.18 and Fig.19) is evident, that Ag dopation has no effect on the phase composition of the samples. The peaks of rutile phase are apparent in the XRD pattern after the calcination, especially after calcination at 400°C. The anatase/rutile phase ratio was calculated using Spurr equation (2) [17]:

$$x_A = \frac{1}{1 + 1.26 \cdot \left( \frac{I_R(110)}{I_A(101)} \right)} \quad (2)$$

where  $x_A$  stand for phase ratio anatase/rutile,  $I_R(110)$  is the intensity of the 110 diffraction peak of rutile,  $I_A(101)$  is the intensity of the 101 diffraction peak of anatase. The anatase (A) rutile (R) content in percents is shown in Tab. 2.

Tab. 2 The anatase rutile percentage content

sample	A (%)	R (%)	sample	A (%)	R (%)
TiO <sub>2</sub>	100	0	Ag-TiO <sub>2</sub>	100	0
TiO <sub>2</sub> -300	70	30	Ag-TiO <sub>2</sub> -300	69	31
TiO <sub>2</sub> -400	68	32	Ag-TiO <sub>2</sub> -400	62	38

Based on the results presented in the Tab. 2 it can be seen that Ag dopation does not significantly affect the anatase/rutile phase ratio. The calcination temperature has positive effect on the formation of rutile phase.

### 3.3.2 Scanning electron microscopy

The morphology of the TiO<sub>2</sub> powder samples was studied using SEM (Philips XL 30). The samples were covered with a Au/Pd film. The SEM images were obtained using a secondary electron detector (SE). The elemental composition of the samples was provided by the Energy-dispersive X-ray spectroscopy (EDX). As mentioned before the theoretical Ag content was 0.21% and this amount is under detection limit of EDX, the presence of titanium was confirmed.

The morphology of the  $\text{TiO}_2$  and the  $\text{Ag-TiO}_2$  samples was very similar. An agglomerate of nanoparticles prepared by drying of the gel prepared by procedure described in chapter 2.1 “Preparation of pure  $\text{TiO}_2$ ” is shown in the Fig. 20. It is clearly observable, that the agglomerates are in the order of tens of micrometers.

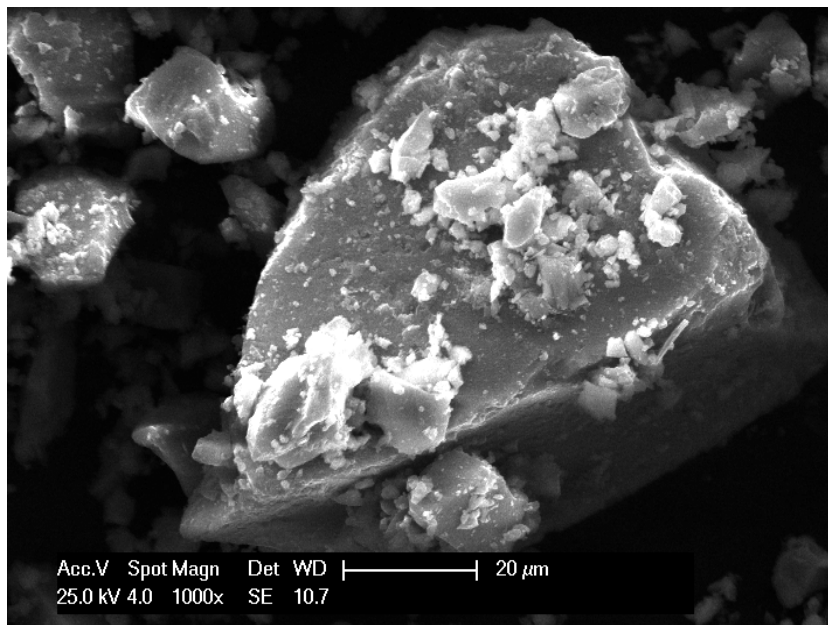


Fig. 20 SEM image of  $\text{TiO}_2$  particle agglomerate.

The SEM proved presence of the particles with dimensions in micrometer rather than in nanometer scale. The experiment when the agglomerates were disintegrated in water into smaller particles showed they are able to pass through the filter with pore diameter  $0,2 \mu\text{m}$  verified the fact that observed agglomerates are formed by significantly smaller particles. It was also observed that the particles did not sediment during a four-day period. This information indicates that agglomerates can be desintegrated into nanoparticles.

### 3.3.3 Atomic force microscopy

The morphology of the films surface was studied using SolverNEXT (NT-MDT) atomic force microscope (AFM) operated in semi-contact mode. It is apparent from the Fig.21 that the calcined  $\text{TiO}_2$  film has smoother surface than the dried  $\text{TiO}_2$  film. The parameters characterizing the surface roughness ( $S_q$  and  $S_a$ ) were calculated using software IA P9 (NT-MDT) and are shown in the Tab. 3.

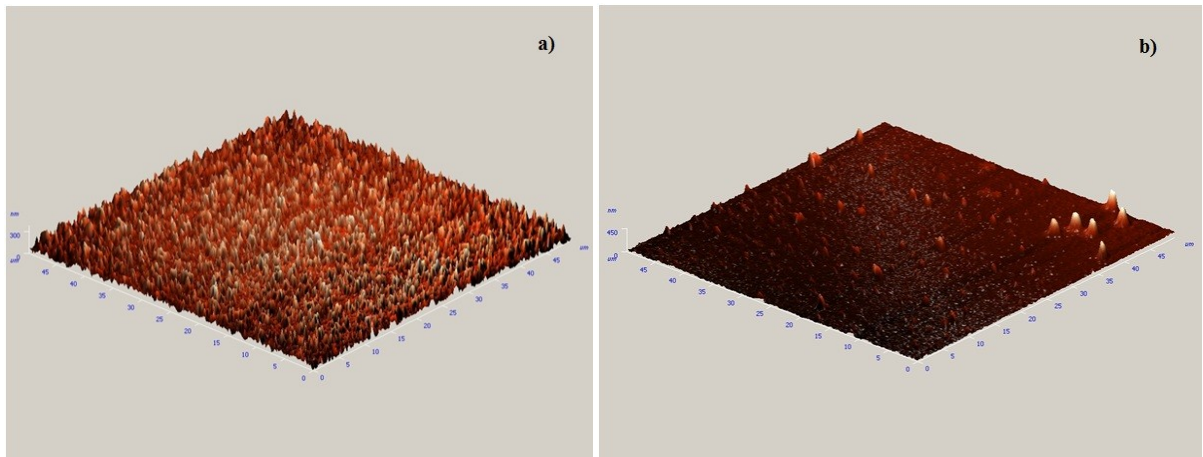


Fig.21 AFM images of  $\text{TiO}_2$  layers a) dried  $\text{TiO}_2$  coated glass b) calcined  $\text{TiO}_2$  coated glass.

Tab. 3 The parameters characterizing the surface roughness.

sample coating	$S_q$ (nm)	$S_a$ (nm)
$\text{TiO}_2$	127.1	116.3
$\text{TiO}_2$ -500	71.8	66.9

The parameters in tab.3 are root mean square roughness ( $S_q$ ) and average arithmetic roughness ( $S_a$ ). From the Fig.21 can be clearly seen that the calcined  $\text{TiO}_2$  film is smoother than the dried  $\text{TiO}_2$  film, this observation is in good agreement with the results published by [18].

### 3.3.4 Raman confocal microscopy

The phase composition of the prepared films was determined using Raman confocal microscopy (XploRA™, HORIBA Jobin Yvon) by spot analysis with green laser  $\lambda = 532$  nm. Raman spectra of the films  $\text{TiO}_2$  and  $\text{TiO}_2$  calcined at  $500^\circ\text{C}$  ( $\text{TiO}_2\text{-}500$ ) for 1h are shown in the Fig. 22.

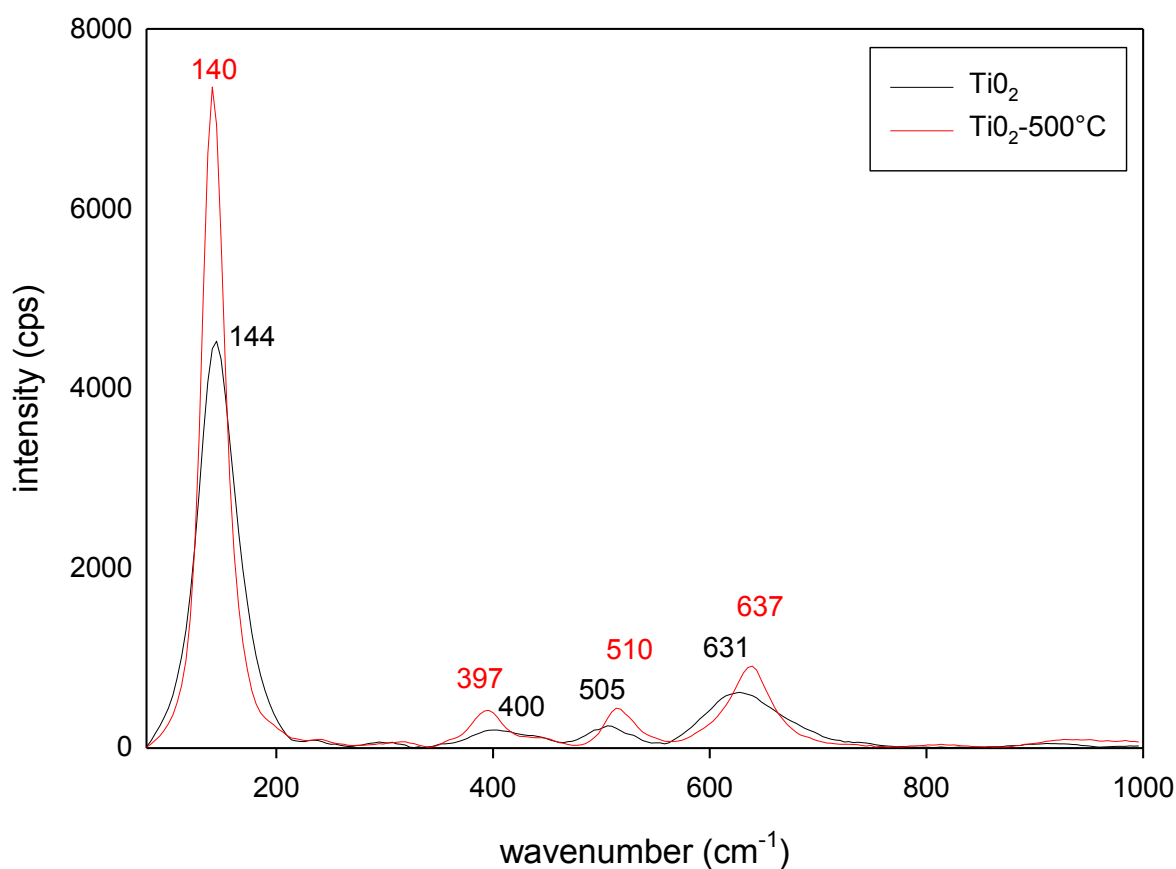


Fig. 22 Raman spectra of the  $\text{TiO}_2$  film and  $\text{TiO}_2$  film calcined at  $500^\circ\text{C}$  ( $\text{TiO}_2\text{-}500^\circ\text{C}$ ).

The characteristic vibration of anatase structure is clearly visible at  $140\text{ cm}^{-1}$  resp.  $144\text{ cm}^{-1}$ . The presence of rutile was not verified.

### 3.3.5 Optical emission glow discharge spectroscopy

The optical emission glow discharge spectrometer GDA750A (Spectro) was used for the verification of Ti presence in the prepared layers and for the characterization of the relative thickness of the prepared layers. The increase in thickness of the films with each layer of TiO<sub>2</sub> is shown in Fig.23. The sample with one layer of TiO<sub>2</sub> coated on glass was named Si-Ti, Si-2xTiO<sub>2</sub> is the sample with 2 calcinated layers of the TiO<sub>2</sub> coated on glass plates, Si-3xTiO<sub>2</sub> is the sample with 3 calcinated layers of the TiO<sub>2</sub>.

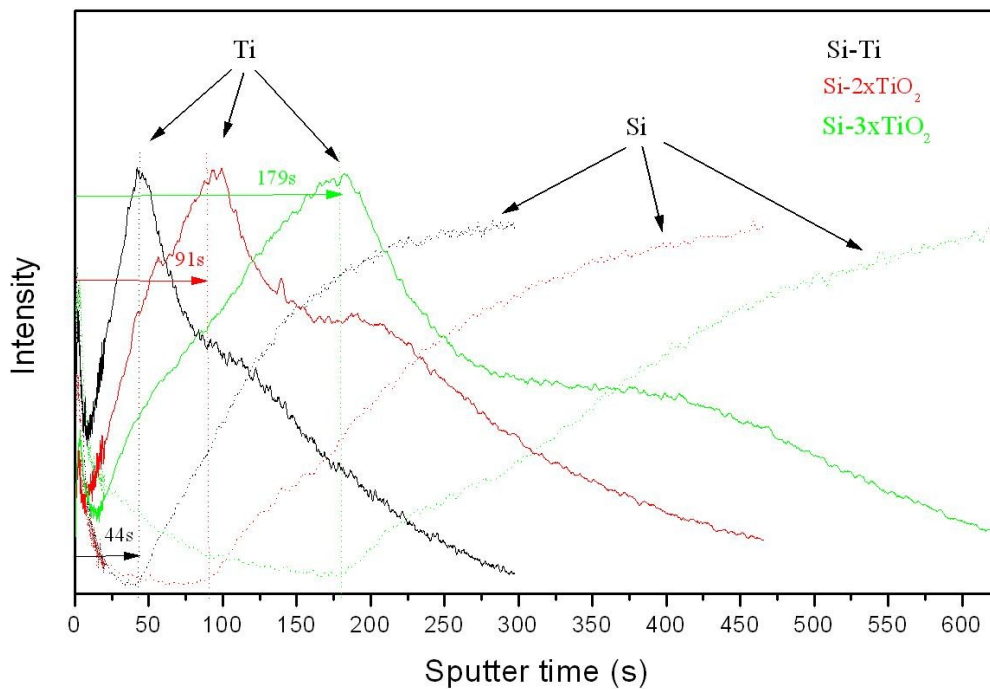


Fig.23 The relative thickness of prepared TiO<sub>2</sub> films determined by OE GDS.

From the Fig.23 is evident that to sputter the pure TiO<sub>2</sub> layer of the sample Si-Ti, Si-2xTiO<sub>2</sub>, and Si-3xTiO<sub>2</sub> took 44 seconds, 91 seconds and 179 seconds, respectively. The increase of the film thickness is not linear with the number of TiO<sub>2</sub> layers. The absolute thickness of the films can be calculated from the sputter time when the suitable standard will be available.

### 3.3.6 Photodegradation activity measurement

Photodegradation activity was evaluated by measuring of the absorbance of the model dye solution. The model dye is degraded by photocatalytic active  $\text{TiO}_2$  after its UV irradiation.

#### *Photodegradation activity of powdered $\text{TiO}_2$*

In the case of the nanoparticles, the prepared sample (50 mg) was mixed with distilled water (65 ml) and acid orange 7 p.a. (Sigma Aldrich) solution (5 ml,  $c=6.10^{-4}$  mol/L). The mixture was stirred in a sealed reactor for 1 hour in the darkness in order to achieve saturated absorbtion of the dye by the powder sample. It is important to let the sample absorb the dye before the sole photodegradation take place because it could misinterpret the measured absorbance data. An UV lamp (UVP, Pen Ray 356 nm ) was placed inside the reactor. Approximately 2 ml of colloid suspension was sampled in 5-minute intervals for the purposes of absorbance measurement. As mentioned in chapter 3.3.2, the desintegrated particles could not be filtered, so the zero absorbance  $A_z$  was set using the colloid suspension of the sample (50 mg) dispersed in distilled water (70 ml) and measured using fiber optics spectrometer USB4000 (OceanOptics) (Fig.24). The absorbance at the start of the measurement in the time 0 min. is designated as  $A_0$ , further measured absorbance is designated as  $A_\tau$ . While measuring the absorbance of the sample, the Pen Ray lamp was placed out of the reactor. After the absorbance measurement the sample was returned to the reactor and the procedure of the UV illumination continued.

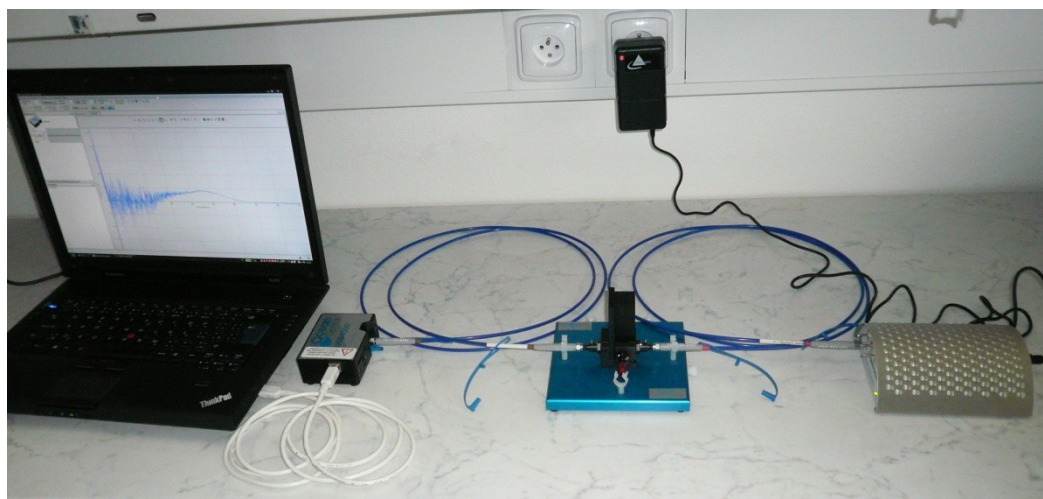


Fig.24 The aparature of the optical spectrometer used for determination of the absorbance of the solution of the model dye and distilled water.

The experiment lasted for 40 min.. After 35 min. exposure to irradiation the decrease in absorbance was approx. 80 % for uncalcined TiO<sub>2</sub> and Ag-TiO<sub>2</sub> samples. The time dependency of AO7 degradation is graphically presented in Fig.25. It is apparent that the extent of photodegradation is lower for the calcined samples.

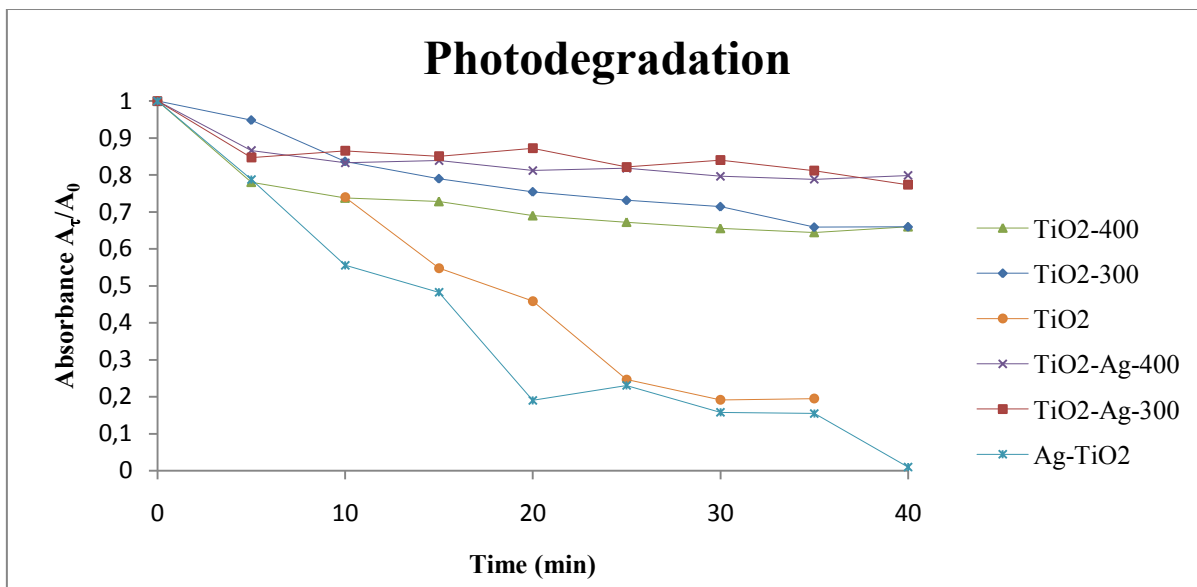


Fig.25 The dye degradation expressed as the  $A_t/A_0$  ratio at wavelength 485 nm.

#### *Photodegradatin activity of thin films*

In the case of thin films, the tubes were coated with TiO<sub>2</sub> and then sealed on one end with glass plate using silicon adhesive. The adhesive was applied on the outer surface of the joint between the tube and the glass to prevent the interaction of the adhesive with the mixture of distilled water (65 ml) and acid orange 7 solution (5 ml,  $c=6 \cdot 10^{-4}$  mol/L). The zero absorbance was set using distilled water, while the absorbance was measured by fiber optics spectrometer (Fig.24). The solution of the model dye mixed with distilled water was subsequently poured into the glued tube. The aparature for photodegradation experiment is shown in Fig. 26. After the insertion of UV lamp (UVP, Pen Ray 356 nm) into the glued tube filled with the model dye water solution, the tube was sealed with aluminium foil to prevent the water evaporation. The aluminium foil was also used to wrap the tube in order to protect the solution against the daylight. From that point the procedure of meassuring photocatalytic activity was the same as in the case of nanoparticles.

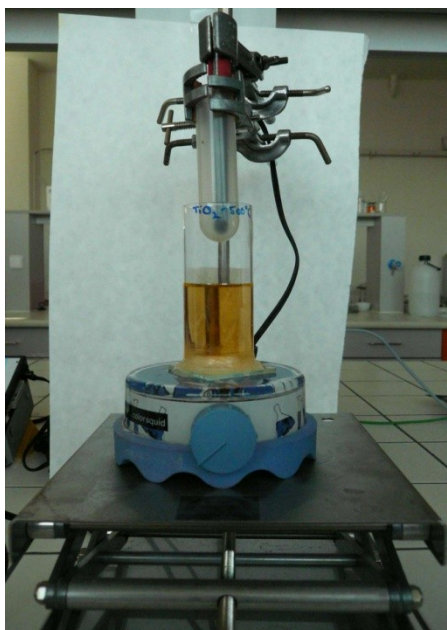


Fig. 26 The photodegradation apparatus used for films.

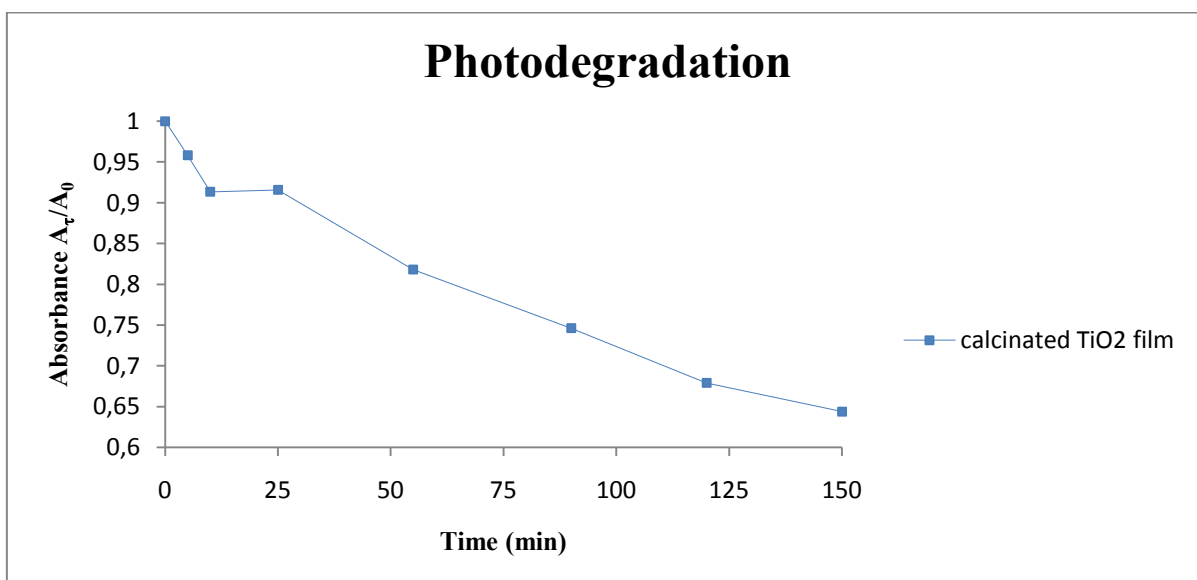


Fig. 27 Dye degradation expressed as a ratio  $A_t/A_0$  at wavelength 485 nm.

The photodegradation activity of dried TiO<sub>2</sub> film coated on bare glass tube showed no significant degradation in the time interval of one hour and the measurement was ended. The photodegradation activity of TiO<sub>2</sub> film coated on bare glass tube and calcined at 500°C for 1 hour is significantly enhanced in comparison to dried TiO<sub>2</sub> films. The experiment lasted for 2.5 h, this exposure to irradiation caused approx. 35 % decrease in initial absorbance  $A_0$ .



## 4 Conclusion

The TiO<sub>2</sub> in the form of powder as well as in the form of thin film was successfully prepared. The method for the measurement of the photodegradation activity of films was developed. The samples prepared in both forms (powder as well as film) exhibited significant photodegradation activity characterized by AO7 degradation. Using the prepared TiO<sub>2</sub> powder 80% degradation of model dye in water solution was achieved after 35 minutes of UV irradiation. Using the calcined TiO<sub>2</sub> film 35% degradation of model dye water solution was achieved after 150 minutes of UV irradiation. The slower photodegradation activity of the film is attributed to smaller surface in comparison with prepared TiO<sub>2</sub> nanoparticles.

The thermal treatment of TiO<sub>2</sub> and Ag-TiO<sub>2</sub> nanoparticles did not improve photocatalytic activity and led to increase in the crystallite size of the both samples. The presence of titanium in anatase form and anatase/rutile ratio was determined by the XRD. The presence of rutile phase was confirmed in the calcined powder TiO<sub>2</sub> and Ag-TiO<sub>2</sub> samples. Experimentally was shown that agglomerates of the particles dissolve in water into submicron particles. The Ag doping had no positive effect on any of the monitored parameters.

Thermal treatment of the TiO<sub>2</sub> film improved its photocatalytic activity and the AFM proved that the calcination smoothed the surface of the film. The presence of the titanium and the relative thickness of the film was determined by OE GDS. The Raman confocal spectroscopy confirmed the presence of the anatase phase in the films.

## 5 Acknowledgments

I would like to thank Ing. Vlastimil Matějka, Ph.D for his guidance, help and will.

Also I would like to thank Marie Heliová (SEM), Pavla Peikertová (Raman microscopy) and Jiřina Vontorová (OE GDS).

## 6 Literature

- [1] HALLAGAN, J.,B.; ALLEN, D., D.; BORZELLECA, J., F.; The Safety and Regulatory Status of Food, Drug and Cosmetic Colour Additives Exempt from Certification. *Food and chemical toxicology*,1995, vol.33, no.6, p. 515-91.
- [2] CARP, O.; HUISMAN, C.,L.; RELLER, A.; Photoinduced reactivity of titanium dioxide. *Progress in Solid State Chemistry*, 2004, vol.32, no.1-2, p. 33-177
- [3] LANG, J.; KALBÁČOVÁ, J.; MATĚJKA, V., KUKUTSCHOVÁ, J.; PREPARATION, CHARACTERIZATION AND PHYTOTOXICITY OF TiO<sub>2</sub> NANOPARTICLES. In *Proceedings of 2<sup>nd</sup> International conference Nanocon 2010, Olomouc 12.-14. October, 2010*. Ostrava:Tanger Ltd., 2010, p. 313-317
- [4] ADDAMO, M.; AUGUGLIARO, V.; DIPAOLA, A.; et al. Photocatalytic thin films of TiO<sub>2</sub> formed by a sol-gel process using titanium tetraisopropoxide as the precursor. *Thin Solid Films*. 2008, vol.516, no.12 p.3802-3807
- [5] LEŠKO, J.; TRŽIL, J.; ULLRYCH, J.; *Obecná chemie*. 2.nd. ed. Ostrava: VŠB-Technical University of Ostrava, 2005, 170 p. Faculty of Metallurgy and Materials Engineering.
- [6] KANEKO, M. ;OKURA, I ; *Photocatalysis: science and technology*. Verlag Berlin Heidelberg New York: Springer, 2002.
- [7] KLEIN, L.;C.; *Sol-gel technology for thin films, fibers, preforms, electronics and specialty shapes*. Mill Road,Park Ridge, New Jersey: Noyes publications, 1988. ISBN 0-8155-1154X.
- [8] HAN, F; KAMBALA, V., S., R.; SRINIVASAN, M.; RAJARATHNAM, D.; NAIDU, R.; Tailored titanium dioxide photocatalysts for the degradation of organic dyes in wastewater treatment: A review, *Appl. Catal.*, 2009, vol. 359, no.1-2, p. 25-40.
- [9] WU, Z.; WANG, H.;LIU, Y.; GU, Z.;Photocatalytic oxidation of nitric oxide with immobilized titanium dioxide films synthesized by hydrothermal method. *Journal of hazardous materials*, 2008, vol. 151, no.1, p. 17-25.
- [10] COLÓN,G.; MAICU, M.; HIDALGO, M.C.; NAVÍO, J.A.; KUBACKA, A.; FERNÁNDEZ-GARCÍA, M.; Gas phase photocatalytic oxidation of toluene using highly active Pt doped TiO<sub>2</sub>, *Journal of Molecular Catalysis A: Chemical*. 2010, vol. 320, no.1-2, p.14-18.

- [11] ISO 22197-1:2007: Fine Ceramics (Advanced Ceramics, Advanced Technical Ceramics) -- Test Method for Air Purification Performance of Semiconducting Photocatalytic Materials - Part 1: Removal of Nitric Oxide.
- [12] ISO 22197-1:2007: Fine Ceramics (Advanced Ceramics, Advanced Technical Ceramics) -- Test Method for Air Purification Performance of Semiconducting Photocatalytic Materials - Part 3: Removal of Toluene.
- [13] LEE, M., S.; SEONG-SOO HONG, S., S.; MOHSENI, M.; Synthesis of photocatalytic nanosized TiO<sub>2</sub>-Ag particles with sol-gel method using reduction agent. *Journal of Molecular Catalysis A: Chemical*, 2005, vol. 242, no.1-2, p. 135-140
- [14] ZITA, J.; MAIXNER, J.; KRÝSA, J.; Multilayer TiO<sub>2</sub>/SiO<sub>2</sub> thin sol-gel films. Effect of calcination temperature and Na<sup>+</sup> diffusion. *Journal of Photochemistry and Photobiology A: Chemistry* 216, 2010, vol.216,p.194-200
- [15] HUANG, Y., Y.; CHOU, K., S.; Studies on the spin coating process of silica films. *Ceramics International*, 2003, vol.29, no. 5, p. 485-493.
- [16] SCHERRER, P.; Estimation of the previous and internal structure of colloidal particles by means of roentgen rays, *Nachr. Ges. Wiss. Gottingen*, 1918, p. 96–100.
- [17] SPURR, R.,A.; Myers, H.; Quantitative Analysis of Anatase-Rutile Mixtures with an X-Ray Diffractometer, *Analytical Chemistry*, 1957, vol.29, no. 5, p 760–762.
- [18] SHARMA, S., K.; VISHWAS, M.; RAO, K., N.; MOHAN, S.; REDDY, D., S.; GOWDA, K., V., A.; Structural and optical investigations of TiO<sub>2</sub> films deposited on transparent substrates by sol–gel technique. *Journal of Alloys and Compounds* , 2009, vol. 471, no.1-2, p. 244–247.